Drying Technology

An International Journal

ISSN: (Print) (Online) Journal homepage: https://www.tandfonline.com/loi/ldrt20

High molecular weight chitosan based particles for insulin encapsulation obtained via *nanospray* technology

Cecilia Prudkin-Silva , Jimena H Martínez , Florencia Mazzobre , Cinthya Quiroz-Reyes , Erwin San-Juan , Eduardo San-Martín & Oscar E. Pérez

To cite this article: Cecilia Prudkin-Silva , Jimena H Martínez , Florencia Mazzobre , Cinthya Quiroz-Reyes , Erwin San-Juan , Eduardo San-Martín & Oscar E. Pérez (2020): High molecular weight chitosan based particles for insulin encapsulation obtained via *nanospray* technology, Drying Technology, DOI: 10.1080/07373937.2020.1806863

To link to this article: https://doi.org/10.1080/07373937.2020.1806863

Published online: 20 Aug 2020.

DRYING TECHNOLOGY
https://doi.org/10.1080/07373937.2020.1806863

High molecular weight chitosan based particles for insulin encapsulation obtained via *nanospray* technology

Cecilia Prudkin-Silva[a], Jimena H Martínez[a], Florencia Mazzobre[b], Cinthya Quiroz-Reyes[c], Erwin San-Juan[c], Eduardo San-Martín[c], and Oscar E. Pérez[a]

[a]Consejo Nacional de Investigación Científica y Técnicas de la República Argentina IQUIBICEN-CONICET, Universidad de Buenos Aires, Departamento de Química Biológica, Facultad de Ciencias Exactas y Naturales, Ciudad Universitaria, Buenos Aires, CP, Argentina; [b]Consejo Nacional de Investigación Científica y Técnicas de la República Argentina ITAPROQ-CONICET, Universidad de Buenos Aires, Departamento de Industrias, Facultad de Ciencias Exactas y Naturales, Ciudad Universitaria, Buenos Aires, CP, Argentina; [c]CICATA Legaría, Instituto Politécnico Nacional, Alcaldía Miguel Hidalgo, Ciudad de México, México

ABSTRACT

The objective of this work was to obtain Chitosan (CS) based particles for Insulin (INS) encapsulation, *via* nanospray drying of a feeding solution containing equal amounts of both components (0.1% w/v total solids content). The process was performed at pH 3 which is out of the range for electrostatic interactions to occur. The analysis involved the nanoparticles (NP) characterization in the solution before drying (pH 3) by dynamic light scattering (DLS) and after re-hydration at different pHs ($3< pH < 11$). The dried product was characterized by Fourier-transform spectroscopy (FTIR), scanning electron microscopy (SEM) and differential scanning calorimetry (DSC). FTIR allowed detecting the chemical groups involved in INS-CS interactions. The encapsulation efficiency of the glassy NP was $62.3 \pm 0.32\%$ as determined by HPLC. Upon powder re-hydration, NP of diameter <200 nm were obtained, with a minority of them exceeding the micron. The change in the shape and temperature of the main endothermic DSC peak and the higher T_g value of the NP would confirm the increase in INS thermal stability when entrapped in a CS matrix. In terms of biological activity an *in-vitro* system was assayed. 3T3-L1 fibroblasts were exposed to INS and Insulin-Chitosan nanoparticles (INS-CS NP). Both treatments showed AKT phosphorylation, which is an indication of AKT activation. The activity of AKT plays an essential role in cell metabolism (lipid and glucose), growth, proliferation, polarity, among others. This activity is a measure of the upstream cell signals, i.e. INS's receptor activity. Phosphorylated AKT was detected during the assay time for INS-CS NP, showing remarkable differences respect to single INS. Nanodrying technology could be used to trap INS into CS matrix keeping the specific hormone functions and protecting it from the hostile conditions of the body.

GRAPHICAL ABSTRACT

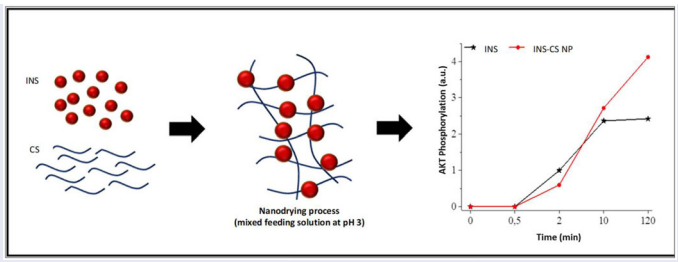

ARTICLE HISTORY
Received 15 November 2019
Revised 7 July 2020
Accepted 4 August 2020

KEYWORDS
nanospray drying; insulin; chitosan; nanoparticles

1. Introduction

Nanospray drying is a technique framed into *Top-down* strategies for NP generation. The process constitutes a clear example of physical entrapment,[1] that allows biomolecules to be introduced into matrices with multiple well-defined properties but without the intervention of chemical processes. The encapsulation *via* nanospray drying protects, stabilizes and enhances solubility, exerting the subsequent controlled release of the bioactive compounds through a powder matrix. Furthermore, the process ensures the microbiological

CONTACT Oscar E. Pérez oscarperez@qb.fcen.uba.ar Laboratorio Interdisciplinario de Dinámica Celular y Nano-Herramientas. Universidad de Buenos Aires, Facultad de Ciencias Exactas y Naturales, Departamento de Química Biológica, Buenos Aires, Argentina.

and chemical stability of the product, by lowering the final water content,[2] and therefore reduces shipping and storage costs. In addition, the efficiency of encapsulation can get up to 90%, assuring particles with reproducible sizes and characteristics.[3]

In general terms, dehydration occurs when the liquid phase, aqueous solution, emulsion or suspension, is atomized in a hot air stream that dries it almost instantaneously. Atomization is achieved by circulating the liquid phase through an atomizer, which can be pneumatic, a pressured mesh, a spinning disk, etc. As the energy increases, the size of the formed droplet decreases. The viscosity and surface tension also regulate the particle size obtained.[4] The time of exposure to high temperatures is usually too small to produce structural damages or activity loss in the compounds of interest, making this technique suitable for thermosensitive compounds such as Vitamin C, whose dehydration and encapsulation into a CS matrix was explained in detail by Gharsallaoui et al..[5] The properties of the polysaccharide greatly influence the result of the dehydration. Such properties determine the particles size, the release time and the efficiency of the drying process. A higher molecular (MW) weight leads to a higher viscosity of the feeding solution and hence irregular-shaped particles are obtained.[6] The deacetylation degree is related with the crystallinity and the hydrophobicity, and the hydrophobic interactions keep relations with the releasing characteristics of these particles.[7] Multiple nano/micromaterials have been obtained by applying the nanospray drying process for increasing protection, bioavailability, physicochemical stability, and maintaining the biological activity of proteins/peptides in a variety of micro and nano-carriers.[8] In this context bioactive compounds such as griseofulvin with antifungal activity,[9] salbutamol encapsulated in lactose (anti-asthmatic drug),[10] resveratrol,[11] folic acid,[12] eugenol,[13] vildagliptin and metformin drugs in mucoadhesive nanoparticles were designed for maintaing the therapeutic drug concentration,[14] even probiotic bacteria and yeast, e.g. *Lactobacillus casei* 01 and *Saccharomyces cerevisiae,* respectively[15] became bioactives for this technique. Interestingly, the spray drying process or some properties of the dehydrated final powder can also be improved by adding additives, such as trehalose or mannitol, able to stabilize pharmaceutical active compounds or to extend shelf life.[9,16] On the other hand, Arabic gum, whey proteins, polyvinyl alcohol, modified starch, and maltodextrin represent a wide spectrum of suitable encapsulating materials.[17] Sodium alginate is often used as an emulsifier and immobilization agent.[18]

The greatest challenge to overcome in the case of traditional spray drying is the high temperatures and/or shear forces at which the suspensions are submitted during the procedure. Thus, the temperatures reached in the dehydration vessel during processing can cause undesirable effects in sensitive proteins and peptides, i.e. inactivation and loss of biological activity of enzymes, physical and chemical modifications such as aggregation, denaturation, oxidation, and even hydrolysis. Further, the adsorption of these species on the device surfaces could also cause the unfolding of native molecular structures. In comparison with the traditional technology, nanospray offers the possibility that samples are submitted to high temperatures during a shorter period and therefore their influence is not usually extensive.[19]

In this work, CS was used as an encapsulating matrix. CS is a biodegradable, biocompatible and non-toxic polymer obtained from chitin. It is known that chitin is a byproduct from fish farms activities that becomes an environmental pollutant. After a chemical modification (deacetylation), chitin is transformed from contaminant to a new product (CS) with added value and new properties. The presence of -NH2 and -OH groups gives CS interesting chemical and biological properties, such as mucoadhesion.[20] Meanwhile, INS is a peptide hormone worldwide used in the treatment of diabetes by INS-dependent patients. In the search for new forms of INS administration, it was reported that oral administration of this hormone has low bioavailability, due mainly to gastric pH and the enzymatic barriers of the intestinal epithelium.[21]

Novel processes were employed to produce INS sub-microparticles from an ethanol/water solution[22] or solvent evaporation. Such processes were designed for diminishing the chances of protein denaturation and to be used in addition to spray drying technique for micro- and nanospheres/particles preparation.[23] Such possible denaturation may arise from exposure to high temperatures or solvents used in traditional drying.

In this context, other routes for INS administration such as the pulmonary, are being explored especially those intended for pediatric patients. This drug delivery route is noninvasive and used for treating a variety of diseases.[24] CS mucoadhesion properties become highly useful in this case. This work is part of a larger project that deals with the encapsulation of INS into CS-based nanostructures. Previously, *core-*

shell NP were designed using the electrostatic complexation principle and their characterization was described in Prudkin-Silva et al.[25]

The objective of the present work was to obtain and characterize CS based nanoparticles for INS encapsulation *via* nano spray drying technology from mixed solutions at pH 3. Under these conditions, the INS entrapment could be promoted into a CS matrix. Such particles will constitute nanovehicles for the protein, exerting protection and enhancing its bioavailability, with a view toward pulmonary route administration.

2. Materials and methods

2.1. Materials

The CS used in this work (MW 300 kDa, deacetylation degree of 72%), was gently provided by the Microbiology Laboratory of Instituto Nacional de Tecnología Industrial of Mar del Plata, Argentina, through the joint project PICT 2015-3866. Recombinant Human INS, was kindly donated by Denver Farma Laboratory, Argentina.

2.2. Methods

2.2.1. Preparation of INS-CS NP via nano-spray drying

The precise amount of CS was dissolved in acetic acid solution (0.05% v/v), under gentle magnetic stirring during 24 h. After that time, CS solutions were submitted to sonication in a bath system at a 25 kHz (Elmasonic TI-H, Elma, Singen, Germany) for 30 minutes. An acoustic power of 100 W was supplied.

The final CS concentration is an important parameter to be considered in the dehydration process. The viscous nature of CS could affect the particle generation process leading to operational malfunctions. Our experimental knowledge indicates that the CS used in this contribution yields very viscous solutions at concentration $\geq$ 1% w/v due to its high molecular weight. As a consequence, its injection in a dryer device would be impeded. For this reason, CS concentrations below 1% w/v were always considered.

INS was dissolved in 20 mM HCl aqueous solution to give a concentration of 0.2% w/v.[26,27] This solution was use as control for the further experiments. The protein solution was kept at room temperature for 2 h to achieve complete hydration before its use.

To prepare INS-CS mixed solutions, a given volume of the INS solution (0.2% w/v) was gently dropped into the equal volume of CS solution (0.2% w/v) under magnetic stirring in order to obtain a final concentration of 0.2% w/v, for each component. The pH of mixed solutions was adjusted at pH 3 before the solution was injected.

A Büchi nanospray dryer device (Nano Spray Dryer B-90, BÜCHI corp., Flawil, Switzerland) with a spray mesh pores of 4 μm diameter was used. The operating parameters were: air inlet temperature (T_{in}) 120 °C, the air flow (GF) was approximately 9.55 kg/h; the oulet temperature (T_{out}) varied between 50 – 55 °C; the internal chamber vacuum pressure was 33 mbar and the solution feeding rate (Fr) was kept in 3 ml/min. The dried powders were collected from the particle collecting electrode using a scraper, and then stored in a desiccator, containing a desiccant material at room temperature for further characterization. The water content was determined by the Karl Fisher titration method, and the result was similar among the different dehydrated samples, 2.0 ± 0.1%, dry basis (d.b.).

The nanospray drying technology has critical variables that define the success or failure of its application, other than the size of the grid, the pressure of the pump or the inlet and outlet temperatures of the drying air stream. Preliminary studies were performed by modifying the process variables to setup the optimal conditions. For example, the mass of the solution to be dried and the fraction of solids injected are also important, since if they were not sufficient, the collected material would be scarce. The sample viscosity is also relevant, hence, the flow inlet and the valve opening must be adjusted in order to ensure that the drying time is adequate for the correct sample deposition,[28] ensuring the physicochemical integrity of the entrapped material and therefore, its functionality. The injection time and the volume of the feeding solution were also considered.

2.2.2. Dynamic light scattering (DLS) and ζ-Potential

Particle size distribution and ζ-potential measurements were carried out using a Zetasizer Nano-Zs particle analyzer (Malvern Instruments, Worcestershire, UK), as proposed by Murueva et al.[29] and Pérez et al.[30] The particle size determination was performed on the mixed INS-CS feeding solution, i.e. before injecting INS-CS mixed solutions (pH 3) into the nanospray dryer. Measurements were also performed in INS-CS NP rehydrated at different pH values (in the range 3–11). This study allowed characterizing the INS-CS NP in terms of size and electrokinetic potential as detailed in Section 3.4. Each measure consisted of 10 runs. All samples were analyzed with an angle of 173°, at 25 °C.

Samples were contained in a disposable polystyrene cuvette. Size distribution, expressed in volume and number, was considered to determine the relative importance of each peak.[31]

The ζ-potential was evaluated from the electrophoretic mobility of particles.[30,32] To this end, a Zetasizer Nano-Zs particle analyzer (Malvern Instruments, Worcestershire, UK) was used. Disposable capillary cells DTS1060, Malvern Instruments, Worcestershire, UK) contained the samples.

For the studies of particle size distribution and ζ-potential variation with pH, 16 ± 0.1 mg of NP powder were dissolved in 50 ml of 1:1, 0.5% v/v acetic acid and 20 mM HCl buffer solution and kept under gentle magnetic stirring for 30 min. Afterward, the solution was kept overnight at 4 °C to avoid any biological contamination. NaOH (0.1 N) was added to shift the pH two hours before the measurements. Measurements were done into the same pH range for size determinations.

2.2.3. Scanning electron microscopy (SEM)

NP powders ultrastructure and morphology were determined by scanning electron microscopy (SEM, JSM- 6390LV, JEOL, Japan). Samples were placed in holders attached to graphite tape and then were covered with a thin layer of gold by a vacuum sputtering (Desk IV, Denton vacuum, USA) process.[33] The edge-to-edge diameter of INS-CS NP was determined by analyzing SEM images ($n = 5$) with FIJI-ImageJ software (NIH). Size-frequency measurements of INS-CS NP were expressed as a histogram.

2.2.4. Ft-IR spectroscopy

Fourier Transform Infrared spectroscopy was used to evaluate the interactions among chemical groups of CS and INS established in NP.[34] FTIR measurements were performed using an Agilent Cary 630 (Agilent Technologies, USA) spectrometer in the range of 4000–400 cm^{-1} with a resolution of 4 cm^{-1} and averaged over 64 scans. Samples were kept in a desiccator 48 h before their use to avoid hydration.

2.2.5. High-performance liquid chromatography (HPLC)

The amount of INS trapped in the NP was measured by the HPLC technique, adopting the protocol presented by Pan et al.[35] The equipment used was an Agilent 1200 series HPLC (Agilent Technologies, USA) with a Quaternary pump G 1315 C and a multiple wavelength detector. To this end, firstly, 2 mg/ml INS, CS or INS-CS solutions were prepared by dissolving each powder in the respective solvent as indicated in Section 2.2.1. Each solution was then passed through a 0.45 μm hydrophilic Millipore Millex HV filter before its injection.

A reversed-phase Zorbax Eclipse Plus C18 (4.6 × 100 mm, 3.5 μm) column was used at 35 °C. The mobile phase was a mixture of acetonitrile: 0.1 M NaH_2PO_4: 0.05 M Na_2SO_4, 30:35:35 (adjusted to pH 3.0 by adding phosphate acid). The flow rate was kept at 0.7 ml/min and the injection volume was 5 μl per sample. Several wavelengths were firstly considered (212, 215, 229 and 276 nm) to minimize the interference from the mobile phase, the acetic acid or CS with the signal corresponding to the INS. Finally, a wavelength of 229 nm was found as appropriate. The corresponding chromatograms were obtained with the Agilent Chem Station software (Rev. B04.01 2009), USA.

To determine the entrapment efficiency (EE), a calibration curve was firstly built using INS solutions containing different protein concentrations. This curve related the Area (A) under the maximum peak with the INS concentration (C) of each injected sample and was fitted according to a standard linear equation ($A = 4491.85 \times C - 515.10$, $R^2 = 0.998$). Hence the HPLC peak area was obtained for the NP powder (2 mg/ml) dissolved at pH 3, and the INS content was determined through the calibration curve. The entrapment efficiency was calculated according to Eq. (1).[36,37]

$$EE = \frac{INS_{NP}}{NP_{powder}} x100 \quad (1)$$

where, INS_{NP} is the concentration of INS determined in a solution of NP powder mass (NP_{powder}) equal to 2 mg/ml.

2.2.6. Differential scanning calorimetry (DSC)

DSC was used to determine the effect of the spray drying process on INS and CS-INS NP thermal behavior. Measurements were carried out using a Mettler Toledo equipment model 822 (Mettler Toledo AG, Greifensee, Switzerland). The instrument was calibrated with indium and zinc.[38] Previous to the measurements, powders of INS and INS-CS NP were placed in a desiccator 24 h at 25 °C. INS powders were set in hermetically sealed aluminum pans (Mettler, 100 μL capacity) and heated from 25 to 260 °C; an empty pan was used as a reference. The heating rate was 10 °C/min under constant purging of nitrogen. The glass transition temperature (T_g) was determined as the temperature at which the change in the specific heat begun (onset value), detected in the

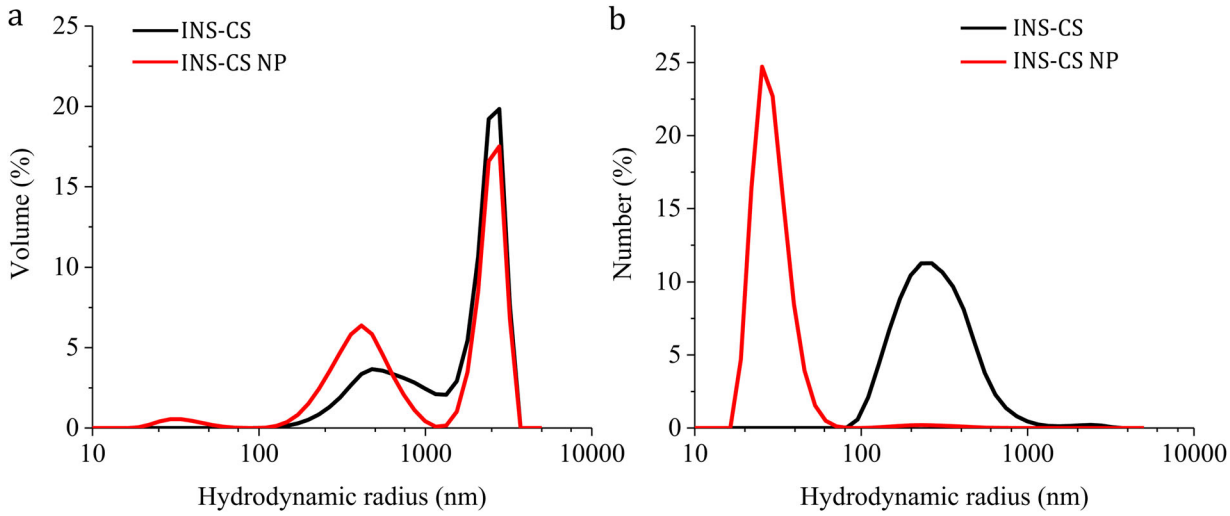

Figure 1. Particle size distribution curves, expressed in volume (a) and number (b), for feeding solution (INS-CS, —) and for resuspended NP solution (INS-CS NP, —) after nanodrying process both at pH 3 and 25 °C. INS-CS NP were obtained by nanodrying the respective feeding solution which had been previously obtained by mixing the appropriate volume of each double concentrated solution of the protein and the polysaccharide (0.2%, w/v), pH 3. Drying conditions: T_{in}: 120 C; GF: 9.55 kg/h and F_r: 3 ml/min.

thermogram as an endothermic shift in the baseline. Temperatures of enthalpic transitions were determined as the peak temperature, and enthalpy values (ΔH, expressed in Jg^{-1}) were obtained by integrating the area below the curve using the Mettler Stare software. All samples were run at least in triplicate and the average of the measured transitions values was reported.

2.2.7. Cell culture and Western blotting

The serine/threonine protein kinase, also known as AKT, constitutes an important pathway in diverse signaling cascades downstream into the cells. This is a result of the upstream signals like INS receptor activation.[39] AKT plays a crucial role in cell survival, proliferation, polarity, and metabolism of lipids and glucose; cell cycle progression; angiogenesis, and others that have been well documented. Also, altered AKT activity has been associated with cancer and other diseases, such as diabetes mellitus, and neurodegenerative diseases. Therefore, AKT phosphorylation as an indication or an application concept, that the biological function of encapsulated INS was maintained into INS-CS NP. American Type Culture Collection, line 3T3-L1 fibroblasts cells were used for the biological essays. Cells were grown in Dulbecco's modified Eagle's medium (DMEM) supplemented with 10% fetal bovine serum (FBS) and penicillin/streptomycin (50 U/ml; 50 mg/ml) (all Gibco; Thermo Fisher Scientific, Inc.). Cultures were grown under the following conditions: 37 °C, 5% CO_2 and 95% of air into a humidified incubator. Western blots were performed according to standard procedures.[25] Briefly, 5×10^4 cells were seeded in plates of 6 wells during 48 h until 70% of confluence. 3T3-L1 fibroblasts cells were serum-starved for 4 h and treated with INS 6×10^{-5}% w/w, or INS-CS NP containing an equivalent INS amount (taking into account the INS trapped into INS-CS NP which was obtained by HPLC), for 0, 0.5, 2, 30 and 120 min. At each time point, cells were scraped in cracking solution (Tris-HCl 200 mM, SDS 8%, Bromophenol Blue 0.4%, Glycerol 40% and β-mercaptoethanol 400 mM), proteases inhibitors (P8340 SIGMA, St Louis, USA) and phosphatase inhibitors (NaF 50 mM, Sodium Orthovanadate 2 mM and β-glycerolphosphate 10 mM) were used. The resulting lysates were run on 10% SDS- polyacrylamide gel and transferred onto a PVDF membrane (Amersham Hybond GE Healthcare Life Sciences, Germany). Blotting efficiency was verified by staining the membrane with Ponceau Red. Membranes were blocked during 1 h with 5% BSA in TBS (150 mM NaCl in 50 mM Tris-HCl buffer, pH 8) solution. After that, the membranes were incubated overnight at 4 °C with a rabbit primary antibody anti-P-Akt S473 1/1000 in 5% BSA in TBS (Cell Signaling, USA). As secondary antibody a Rabbit IgG-HRP 1/5000 in 5% BSA in TBS (Santa Cruz, CA, USA) was added to the membrane and incubated during 1 h at room temperature. Inmunoreactive bands were detected by chemiluminescence with ECL Prime Western Blotting Detection Reagents RPN 2232 (Amersham GE Healthcare, UK) and by using the LAS 1000 plus Image Analyzer (Fuji, Tokyo, Japan). Quantitative changes in protein levels were evaluated with the FIJI-Image J software (NIH). To confirm equal protein

loading in each lane, antibodies were stripped from the membranes with stripping buffer (15% H2O2 in TBS) and re-probed with a loading control [Akt 9272 (Cell Signaling, USA); Rabbit IgG-HRP (Santa Cruz, CA, USA)]. The molecular weight of proteins was estimated by electrophoresis using protein markers as reference (Fermentas Life Sciences, CA, USA).[40]

3 Results and discussion

3.1. Particle size distribution and ζ-potential for feeding solutions and for the re-hydrated INS-CS NP

Particle size distribution and its derived parameters, main peaks, and ζ-potential measurements were obtained using the DLS technique under the conditions proposed by.[30] Figure 1 shows the particle size distribution for the feeding solution (INS-CS) and for the resuspended NP solution (INS-CS NP). The particle size in the feeding solution should be determined, as it has been recently reported and described that the charge regulation mechanism occurs in the system constituted by INS and CS.[41] This mechanism should not be ruled out, especially for pHs that render both species with the same net charges or at pH values that are too close to the isoelectric point of the protein (pI). The phenomenon can be considered as a previous phase to complexation or an incipient complexation stage, somehow equivalent to weak interactions of Coulombic nature, having as a result the intermolecular self-assembly. For this reason the occurrence of *regulation of charges* cannot be dismissed between INS and CS in the feeding solution bosom, therefore particle size expressed in volume was firstly considered. The distribution resulted bimodal in both cases before and after drying (Figure 1a). Two peaks below 1 μm were identified with maximums at 300 and 1100 nm for the original solution and 31.7 and 412.5 nm after the nanodrying process. When the distribution was analyzed in terms of Number (Figure 1b), the representation indicated that the majority of particle number possessed hydrodynamic radii below 100 nm in the re-hydrated material. The results show a peak displacement to smaller particles sizes after drying, which could be attributed to the higher forces acting in the atomizer device. Previous reports attributed this effect to the structure contraction after dehydration, as evaluated by particle size distribution in re-hydrated samples.[42] In this way, a new particulate structure arises after the nanodrying process with a smaller size than those formed by simply protein-polysaccharide association in the bulk of mixed solution, i.e. in the liquid feeding before drying. Such differences are shown in Figure 1a and b.[25]

As far as we know, there are no previous works concerning nanospray dried NP formed with high molecular weight CS, like the one used here for INS entrapping. In fact, literature is abundant regarding other small molecules employed in nanospray drying particle generation. For example, Yang et al.[43] have described the use of histidine, leucine and arginine as excipients for nano dehydration of aztreonam (AZT), due to the ability of these amino acids to modify the morphology, density, humidity content and lung deposition of this nanoparticles.[44] In line with this works, other researchers reported casein nanoparticles construction, designed as a folic acid vehicle.[45] Another small molecule encapsulated by nanospray technology was curcumin.[46] In that interesting work, different process conditions were examined to evaluate the effect that different process variables could have in the final particle size, such as mesh size, CS concentration, the use of surfactants and drying air temperature.[46]

Polysaccharide concentration results of great importance to achieve the desired NP sizes *via* nanospray drying technology. The use of diverse molecular weight CS was reported, which were dissolved in an aqueous media with concentrations ranged from 0.025% w/v[47] to 10% w/v[48] for obtaining particle diameters of around 500 nm. Our results indicated that the smallest NPs were obtained for a CS concentration of 0.1% w/v, and without the use of surfactants or additives. In line, Lee et al.[49] generated nanodryed particles using Bovine Serum Albumin (BSA) as a model protein. The authors also considered the influence that factors such as mesh size, drying temperature or the use of surfactants have in the results. Sphericity was associated with increasing concentrations of surfactant and the particle sizes obtained ranged from 0.5 to 2 µm.

In the present contribution, the nanospray process yield considering the total mass of solids injected and the total amount of particles collected reached 93% for a 1:1 INS-CS solution and a total biopolymer concentration of 0.2% w/w.

The electrochemical potential known as ζ-potential, which is the electric potential operating in the plane of a charged particle during electrophoretic movement,[50] is an important and useful indicator to predict and control the stability of colloidal suspensions. ζ-potential for the original INS-CS liquid feeding, i.e. before drying at pH 3, resulted equal to 59.3 ± 2.2 mV.

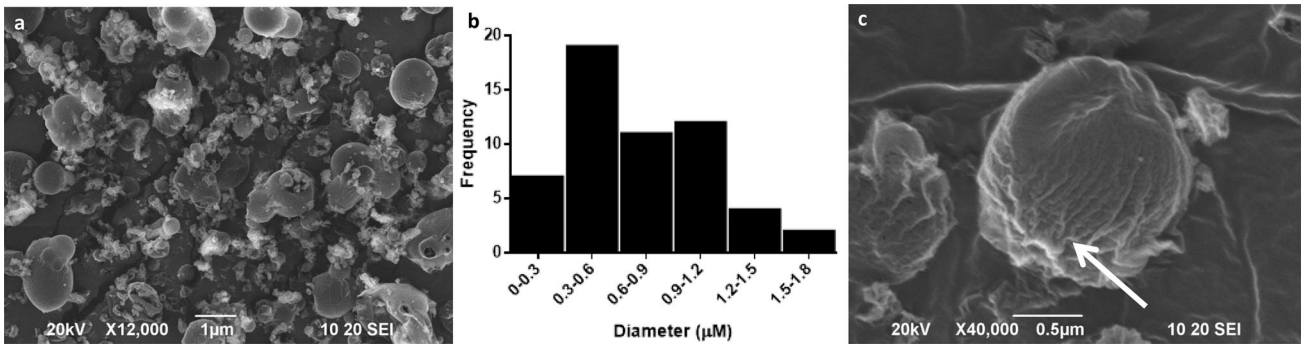

Figure 2. SEM micrographs of INS-CS NP obtained by drying a feeding solution containing equal volumes of protein and polysaccharide of the same concentration (0.2%, w/v) at pH3. General aspect of NPS with spherical beads-like surfaces (a). Particle size distribution of nanodried INS-CS NP obtained by image analysis (b). INS-CS NP aggregates exhibited a striated surface, as indicated by the arrows (c). The scale bar is included in every micrograph. Drying conditions: T_{in}: 120; GF: 9.55 kg/h and F_r: 3 ml/min.

These high ζ-potential values are indicative of high colloidal stability for these mixed solutions. According to the DLVO theory, high electrokinetic potentials result in high electrostatic repulsion between particles, which leads to high colloidal stability.[51] Meanwhile re-hydrated INS-CS NP displayed ζ-potential equal to 25.1 ± 0.5 mV at pH 3. ζ-potential variations could obey to the fact that upon drying, a new structure was formed from the protein and the polysaccharide mixed feeding solution. Thus, charged groups would acquire a particular spatial distribution, different from the one present in the original solution. Concerning to this point, literature indicates that electrostatically stabilized hydrocolloids commonly possess ζ-potentials exceeding absolute values of 40 mV.[52] As no precipitation was seen in the re-hydrated samples, the physical stability of INS-CS NP in solution could not be explained only by electrostatic stabilization, suggesting that other forces contribute to the systems stability. This could stem from hydrophobic interactions, van der Waals interactions or steric overlap interactions.[30] In other words, the physical stability of INS-CS NP in solution depends strongly on the balance between attractive and repulsive interactions between them, given by the surrounding media pH and their interactions with co-solutes. The conformation of the secondary and tertiary structure in the case of the protein forming part of NP and the spatial configuration adopted by the CS[53] are also influential factors.

3.2. Ins-CS NP powders characterization

3.2.1. Ultrastructure

Figure 2a shows SEM images of INS-CS NP powder obtained by nanodrying of the mixed protein and CS solution at pH3. Some spheroid submicron NP and aggregated structures, i.e. microparticles (diameter > 1 μm) can be observed from SEM images. However, the majority of particles felt into the nanoscale (diameter < 1 μm). Particles presented isolated without connecting fibers between them. The micrographs show less uniform field of particles, in terms of appearance, than those CS-based NP reported by Arpagaus et al.[54]

Approximately 50% of NP had a diameter <1 μm, a 12% felt into the range 0.9–1.2 μm and the rest resulted larger than 1.2 μm (Figure 2b).

Although SEM micrographs showed micrometric dimensioned structures (macromolecular aggregates), these could be easily separated, because when in solution INS-CS NP behaved as elucidated by DLS, with particle sizes around 200 nm. Micrometric sized structures formation as a consequence of spray drying has been previously reported for other authors and supported with SEM images,[55,56] with the consequent microparticles formation (diameter ≥ 1000 nm) from NP aggregation. The surface of these structures resembles a string of spherical beads, in contact one with another, with a loss of their sphericity due to the forces and deformation experimented by drying droplets during the dehydration process. In general terms, micrometric sized structures exhibited a striated surface (Figure 3c). This feature can be useful as the striated surface is equivalent to a high rugosity, which in turn increases particle dispersion capacity.[55] On the other hand, rugosity diminishes the possibility of interaction with other particles, reducing interaction forces between particles and therefore increasing the powder dispersion and powder flow capacity.[57]

3.2.2. Ftir

To determine possible interactions among INS and CS in the nanoparticles FTIR spectra were obtained (Figure 3). The spectra corresponding to single INS and CS are shown superimposed with that of INS-CS NP. INS kept its characteristic peaks after dehydration, which were detected at 1647 and 1537 cm^{-1} and

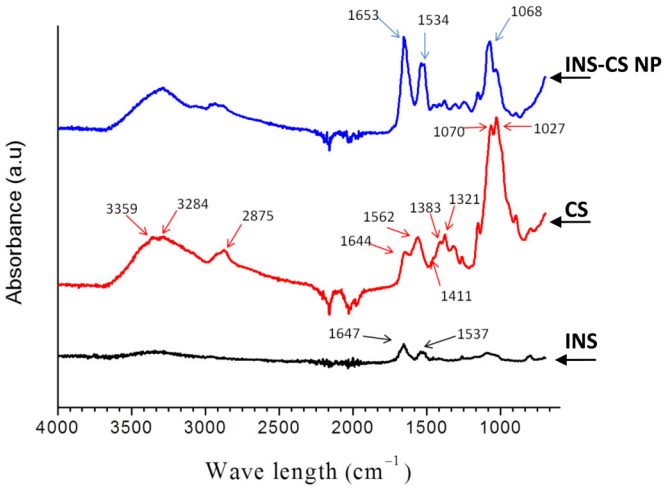

Figure 3. The infrared spectrum of INS, CS and INS-CS NP powders obtained by nanospray drying process in the field 4000–500 cm^{-1}, 25 °C. INS-CS NP were obtained by nanodrying the respective feeding solution which had been previously obtained by mixing the appropriate volume of each double concentrated solution of the protein and the polysaccharide (0.2%, w/v), pH 3. Drying conditions: T_{in}: 120; GF: 9.55 kg/h and F_r: 3 ml/min.

corresponded to Amide I, C = O stretching and Amide II, C–N stretching and N–H bending.[36] The peak obtained at 1647 cm^{-1} can be assigned to the existence of α-helix in the protein structure, as was previously reported.[58]

The CS spectrum exhibited characteristic peaks around 3359 and 3284 cm^{-1}, corresponding to O–H and N–H stretching. The peak at 2875 cm^{-1} was associated with the C–H stretch. The peak detected at 1644 cm^{-1} was assigned to Amide I, C = O. The peak around 1562 cm^{-1} corresponds to the bending of the amine NH-R group (Amide II). At 1383 and 1321 cm^{-1} the peaks corresponding to the CH_3 symmetrical deformation were identified. Meanwhile at 1411 cm^{-1}, the deformation of C–H and O–H in Amide II were detected and in 1070 and 1027 cm^{-1} the signal for the glycosidic bond (C–O–C) was found.[59–62] INS-CS NP spectrum presented three peaks of interest at 1653, 1534 and 1068 cm^{-1}. The first one could be assigned to a combination of signals from CS Amide I and INS Amide II (C = O). The second one presented the combination of Amide II signals from both species, and the third one belongs to the glycosidic bond on CS. INS-CS interaction also provoked a decrease in the signal assigned to the CH_3. Furthermore, the signal corresponding to C–H and O–H was also reduced.

Recently, we informed the FTIR spectra for INS-CS dehydrated material obtained via freeze drying,[41] where no remarkable changes were found for the CS and CS-INS solids. The peaks found in FTIR profile for lyophilized samples would indicate "loose contacts" between the protein and the polysaccharide macromolecules in dilute solution. In line, Boonsongrit et al (2008)[63] reported a minor change in the FTIR spectra of INS–CS microparticles prepared with different concentrations of protein and under acidic conditions, pH 3 and 5. The authors used CS with a MW of 150 kDa and a degree of deacetylation equal to 84.5%. No band shifts could be detected in the FTIR spectra of INS–CS microparticles. However, the author found some CS overlapping bands with those of INS which resulted in a widening of the carbonyl (1654 cm^{-1}) and amine bands (1540 cm^{-1}). This band widening was more distinct with increasing concentrations of INS. In addition, the change of the three small bands at wavenumbers about 1400–1500 cm^{-1} to two bands of INS was also detected. These observations would indicate weak interactions (*loose contact*) among INS and CS molecules which were subsequently confirmed by isothermal titration calorimetry studies.

From the comparison between the reported spectra in Prudkin-Silva et al[41] and those shown here some other discrepancies arise, which could be attributed to intrinsic biopolymers solutions factors as pH, ionic strength and the relative biopolymer concentrations. The drying methods would also have a critical impact on these differences in FTIR results, as reported in literature for spray drying *vs* spray freeze drying,[61,62] freeze, hot air and vacuum drying[64,65] and spray drying *vs* microwave assisted freeze drying.[66]

It is important to note that CS-based encapsulation systems reported in literature, usually involved CS of low molecular weight (<100KDa). For instance, a protein was added into aqueous mixtures containing CS-Tripolyphosphate (TPP)-Vitamin C.[67] Other examples include CS-Tween 80- Mangiferin,[68] CS-Mannitol-Calcitonin,[69] etc. The reader should take into account that the examples cited are ternary systems. This situation renders any comparison not easy for an extended discussion, considering that the mixture presented in this contribution is binary and the MW of the CS is higher than those used in the cited works.

3.2.3. Thermal events. Differential scanning calorimetry (DSC)

DSC offer the possibility of investigating in the same measurement the glass transition temperature of the matrix and the thermal stability (thermal denaturation) of the encapsulated protein.[67]

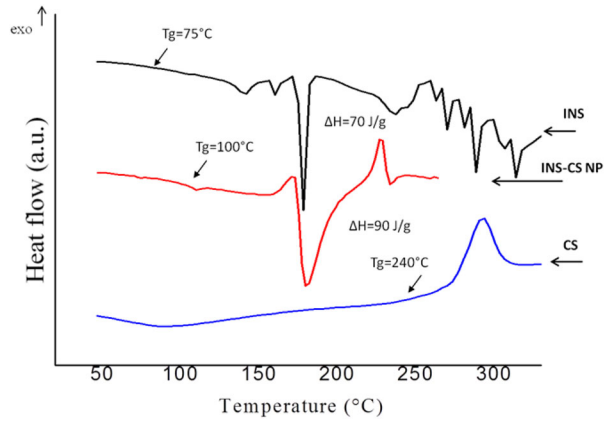

Figure 4. DSC thermograms for INS, CS and INS-CS NP powders obtained by nanospray drying process. For INS-CS NP the nanospray feeding solution was prepared by mixing equal volumes of protein or polysaccharide solutions (0.2%, w/v) at pH 3. Drying conditions: T_{in}: 120 C; GF: 9.55 kg/h and F_r: 3 ml/min. Heat flow is express in arbitrary units (a.u.).

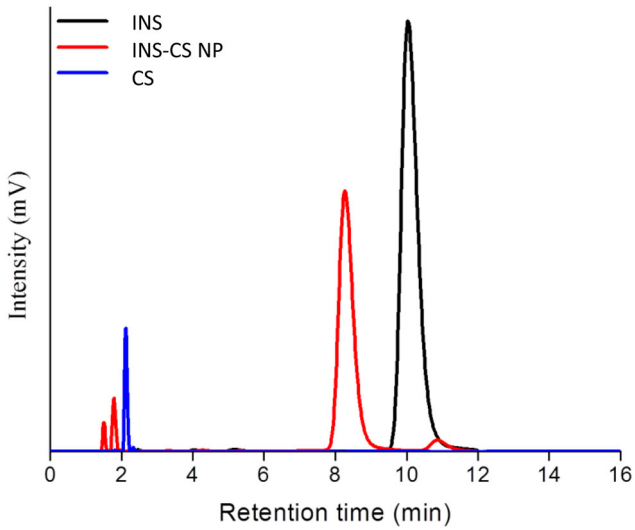

Figure 5. Chromatogram showing elution time for INS, CS, and INS-CS NP, at $\lambda = 229$ nm. This analytical methodology was applied for determining INS in the NP_{powder}. INS-CS NP were obtained by nanodrying the respective feeding solution which had been previously obtained by mixing the appropriate volume of each double concentrated solution of the protein and the polysaccharide (0.2%, w/v), pH 3. Drying conditions: T_{in}: 120; GF: 9.55 kg/h and F_r: 3 ml/min.

In order to evaluate the physical state of the INS-CS NP powder and its thermal transitions, DSC thermograms were obtained for the nanoparticles and for INS and CS powders alone as reference (Figure 4). The DSC thermogram for pure CS exhibits one broad endothermic peak at 110 °C associated with the evaporation of bound water as reported by Adamiec and Modrzejewska,[70] then a glass transition (T_g) near 240 °C and finally an exothermic peak at about 320 °C, attributable to the polymer degradation. This includes saccharide rings dehydration, depolymerization, and decomposition of deacetylated and acetylated chitosan units.[69] The observed peaks are in agreement with others reported studies. For INS, a main endothermic transition was detected at 175 °C that would correspond to the denaturation of the main protein fraction. The peak resulted well defined and sharp, which is in accordance with the high purity of the studied INS (recombinant, of medicinal and analytical grade). High temperatures of denaturation were also reported by other authors for INS with low moisture content, measured under thermal conditions similar to the present work.[71] This high temperature transition was endorsed by the low water content and the predominant INS conformation in associated units. In addition to the main endothermic peak at 175 °C, the INS thermogram shows a small endothermic transition at 130 °C, and an endothermic peak of decomposition at a temperature greater than 220 °C. Since it is known that thermal denaturation in the solid state occurs only at very high temperatures and therefore has no obvious direct relationship to practical stability behavior, the glass transition temperature is commonly measured in protein formulations in an attempt to predict stability.[72] The endothermal baseline shift near 70 °C represents the glass transition temperature (Figure 4). The observed step, accounting for the change in the heat capacity of the material at T_g, is small and spreads over a very large temperature range, as generally reported for most amorphous proteins.[73] This was attributed to a decoupling of the protein internal motions[74] from the motions that characterize whole molecule diffusion and viscous flow. Thus, in protein or protein-rich systems, the glass transition is not the onset of mobility within the protein molecule but rather signals onset of whole molecule rotation and translation.[73]

The thermogram corresponding to the INS-CS NP shows a wider main peak than the one observed for INS and at a slightly higher temperature (180 °C). The enthalpy variation (ΔH) associated with this transition was 90 J/g, greater than that determined for the INS alone (70 J/g), which reflects that more energy is required for INS denaturation into the complex, reinforcing the hypothesis of the thermo-protective effect of CS during the dehydration process. The exothermic peak observed for the CS at high temperature is maintained in the INS-CS NP thermogram. The glass transition temperature for INS-CS NP was around 95 °C, higher than the T_g of single INS but lower than that of CS.

Bellavia et al.[75] working with different protein-trehalose amorphous systems, found a linear relation

Table 1. Main peaks obtained from particle size distribution expressed in volume and ζ-potential values for rehydrated INS-CSNPS, 3< pHs <11, at 25 °C. ND: Not Determined.

pH	Peak1(nm)*	Peak2 (nm)*	ζ Pot (mV)*
3	63.8 ± 22.1	590.7 ± 171.2	25.1 ± 0.5
4	47.2 ± 7.8	612.0 ± 87.9	21 ± 0.7
5	45.9 ± 15.3	431.4 ± 50.1	8 ± 0.6
6	37.8 ± 9.2	396.8 ± 26.7	9.6 ± 0.7
7	119.5 ± 4	910.0 ± 40.1	−11.1 ± 0.6
8–9–10	ND	ND	ND
11		1753 ± 122.3	−4.2 ± 0.4

*mean ± SD, $n = 3$ independently prepared samples.

between the glass transition temperature of the whole matrix and the denaturation temperature of the embedded protein, and suggested that collective water-matrix interactions responsible for the glass transition, also influence the protein stability, with the stabilization extent depending on the specific protein matrix interactions. The fact that a single T_g was evident in the INS-CS NP system (Figure 4), indicates that the components (in this case buffer-protein-CS) form a single amorphous phase which is beneficial for protein stability.[73] To sum up, the employed nano-spray process conditions allowed obtaining amorphous protein-CS particles. In these systems the changes in the shape and temperature of the main endothermic peak with respect to the protein alone, and the higher T_g value suggest an increase in INS thermal stability when entrapped in a CS matrix.

3.3. Quantification of INS in NP

Figure 5 shows the chromatograms obtained for INS and CS individual solutions and for re-hydrated INS-CS NP. The amount of INS determined by HPLC in a NP_{powder} solution of 2 mg/ml was 1.246 mg. Therefore, the EE resulted equal to 62.3 ± 0.32%. Other authors reported EE values > 87.4% for INS loaded CS based NP prepared by ionotropic gelation with tripolyphosphate anions,[76] a different NP formation principle than the used here.

Nevertheless our findings are promising according to the recent report of Hu and Luo,[77] where a complete compilation in terms of the loading capacity of polysaccharide-based particles was offered. For instance, a loading efficiency of 15.7% was obtained for core-shell alginate - CS-based NP. Then, a loading efficiency of 33.0% was informed for a system constituted by a water-soluble CS derivative premixed with INS. On the other hand, Mukhopadhyay et al.[37] designed particles by directly mixing equal volumes of CS and INS solutions with a protein loading efficiency of 39.2%.

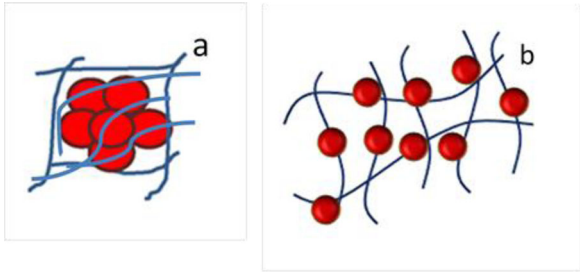

Figure 6. Possible configurations adopted by INS-CS NP after rehydration at different solution pH values. Core-shell type INS-CS NP predominated at pH 6. Cluster type INS-CS NPS were predominant at pH ≤ 5 and pH > 6. Drying conditions: T_{in}: 120; GF: 9.55 kg/h and F_r: 3 ml/min.

Several factors can exert influence on the protein-polysaccharide interactions, as initial protein concentration in solution, pH media or CS characteristics. Thus, Pan et al.[35] found that the encapsulation efficiency of CS based NP crosslinked with TPP was affected by the INS concentration in solution and the amount of INS incorporated. Increasing ratio of INS to CS leads to a slight decrease in association efficiency and an enhancement of loading capacity. In a former work,[78] it was indicated that the encapsulation efficiency of BSA was affected by the initial BSA concentration, the lower the concentration, the higher the encapsulation efficiency. The pH of the NP during the formation process was reported as an influencing factor on protein-polysaccharide interactions, i.e. a pH that favors electrostatic interactions will lead to the entrapment of higher amounts of protein. The authors reported that the CS-enzyme interactions were affected both by the enzyme concentration in NP and on the CS source (shrimp or fungal).

3.4. Study of INS-CS NP stability upon re-hydration at different pH values as evaluated by particle size and ζ-potential

Most of pharmaceutical INS delivery systems require the knowledge of their stability, i.e. particle size with pH variations. Therefore, it is important to understand how INS-CS NP behaved when this variable was under consideration. Table 1 summarizes the principal peaks derived from particle size distribution upon re-hydration with pH solutions ranging between 3 and 11. This pH range included the INS isoelectric point (pI 5.5) and the pH range in which the electrostatic interactions between INS and CS would be favored, from 5 to 6. First of all, it is worth noting that the particle size distribution was bimodal in all cases. A gradual decrease in particle size can be observed as the pH increase from 3 to 6. Just at pH 6 the

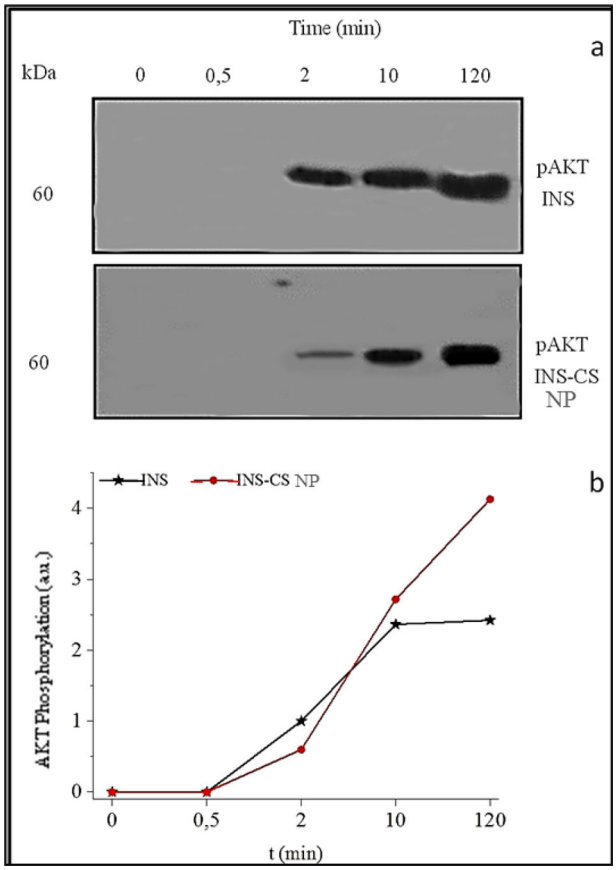

Figure 7. Western blot showing changes in phosphorylated AKT levels after INS or INS-CS NP stimulation, assayed in 3T3-L1 fibroblasts upon a time (a). Quantification of AKT phosphorylation over time showing a sustained increase for INS-CS activation after two hours of stimulation (b). INS-CS NP were obtained by nanodrying. The respective feeding solution which had been previously obtained by mixing the appropriate volume of each double concentrated solution of the protein and the polysaccharide (0.2%, w/v), pH 3. a.u: arbitrary units. Drying conditions: T_{in}: 120; GF: 9.55 kg/h and F_r: 3 ml/min.

electrostatic interactions between INS and CS reach their maximum.[25] Figure 6 shows the configuration proposed for this INS-CS NP structure acquired after NP powder re-hydration at different pH solution. NP would constitute matrices or networks were the INS would be trapped. These matrices would form more open structures at pH values where electrostatic interactions would not be favored (pH $\leq$ 5 and pH $>$ 6) as indicated by the higher particle sizes (Figure 6a and Table 1). These matrices or networks would constitute tighter or more closed structures at pH 6 were the electrostatic interactions were predominant in the system (Figure 6b and Table 1) with the concomitant particle size decrease. In conclusion, different structures with different degree of crosslinking between CS and INS would be obtained as a function of the re-hydration solution pH.

In the field of the pharmaceutical industry and in the study of biological systems of cells and NP, it is worth mentioning that cells within the human body vary from 1 to 100 μm, and therefore, have a low probability of internalizing particles of $\sim$100 μm. The highest rates of endocytosis for smaller sized NP (100 nm) would promote higher bioavailability of the endocytosed carrier.[79] In line, previous reports postulated that NP were highly internalized having sizes ranged 50–100 nm.[80] On the contrary, from a cellular uptake experiments of thio-organosilica NP with 50–500 nm, Awaad et al.[81] concluded that 95–200 nm was the ideal size for cellular uptake increase.

At pH $<$ 6, INS-CS NP presented positive ζ-potential values registering the highest at pH 3 (Table 1). At pH 5 and 6, ζ-potential manifested positive in terms of charge even lower in absolute values. Cluster type NP would have the highest colloidal stability in solution[49] under this condition. It is important to note that ζ-potential informed in[24] for core shell type NP at pH 6 resulted coincident with the value informed here.

ζ-potential for NP re-hydrated solutions at pH $>$ 6 resulted negatives as both, INS and CS, presented this charge under this condition. The study of re-hydrated NP resulted impossible to perform when pH ranged 8–10 as the CS tends to self-aggregate or self-assemble, increasing the particle sizes and favoring the NP aggregation and even precipitation proceeded.[74,75] ζ-potential determinations for pH $>$ 8 were not reliable, as indicated by the phase plot given by the DLS software. Finally, at pH 11, the results manifested a clear trend toward negative. The noticeable CS's low solubility under basic conditions would have an undeniable impact on future technological applications.

3.5. Biological activity of INS determined as AKT effector stimulation

AKT phosphorylation is an evidence of AKT activation which in turn is an indication that the biological activity of INS was maintained in the INS-CS NP. AKT activity is involved in cell metabolism (lipid and glucose), proliferation, polarity, among others. This activity is a measurement of the upstream cell signals, i.e. INS's receptor activity. Thus, to evaluate the biological activity of entrapped INS, changes in phosphorylated AKT levels in cultured 3T3-L1 fibroblasts were registered *via* Western blot at different times after protein phosphorylation induction (Figure 7a).

3T3-L1 cells are pre-adipocytes and after differentiation adopt adipocytes phenotypes. Both phenotypes are able to express both isoforms of INS receptor, A and B, at equal levels.[82] INS receptor activity can be measured through AKT phosphorylation, like was demonstrated by Chen et al..[83] The INS-regulated phosphorylation events are often on serine residues. In 3T3-L1 cells, the percentages have been quantified as 87.8% phosphoserine, 11.4% phosphothreonine and 0.8% phosphotyrosine. In 3T3 cells, the phosphorylation of AKT occurs on Ser473 within one or more minutes and stabilizes.[84] Our results showed that phosphorylation of AKT appear at 2 min after INS exposure.

This experiment confirmed in the first place the structural and functional stability of INS into the CS matrix upon the nanospray drying process. AKT stimulation with both, INS and INS-CS NP, presented a sustained increase up to 10 min, although, free INS stimulation exposed much more modulated or linear behavior into this frame of time (Figure 7b). Such differences can be credited to the fact that after nanospray drying, INS is physically confined in the CS nanoparticle. This network requires a certain amount of time to disentangle, time enough for allowing INS to become in contact with 3T3-L1 cells INS receptors. At times higher than 10 min, the AKT activation demonstrated a remarkable difference for INS-CS NP, with the receptor activity continuously increased.

Interestingly, Prudkin-Silva et al.[25] reported a different AKT activation kinetics for the case of INS-CS NP obtained via electrostatic interaction. The covering of INS by a shell of CS would explain the delayed activation of its cellular response, with no instantaneous access to cell receptors and sustained activation. INS-CS NP obtained *via* nanospray could be considered as polymeric networks or entanglements, but not with the same configuration as the core-shell type NP. From a physical point of view, the similar AKT delayed activation profile could be associated in this case with the swelling behavior of CS and the network disentanglement. The swelling behavior of CS determines the penetration rate of water inside the polymer network. Usually, hydrophilic polymers such as CS, swell when in contact with an aqueous medium. In general terms, these phenomena can be influenced by the nature of the encapsulating material and the conditions of the swelling medium: pH, ionic strength and temperature.[85]

The delayed phosphorylation of AKT provoked upon INS-CS NP stimulation, in comparison with single INS stimulation could also be explained from a chemical point of view. Under physiological conditions, pH 7.4 and a temperature of 37 °C, CS's amino groups and the INS carboxyl groups would start to lose their electrostatic interactions, thus allowing the intrusion of water molecules inside the polymeric network.[86] In terms of size, NP would have enormous importance as a carrier system at cellular level and a significant role in drug delivery. For instance, in the case of tumors, it was reported that NP can be accumulated in the microenvironment. This is due to the enhanced permeability and retention effect and can offer long blood circulation; because NP cannot be easily recognized by the reticuloendothelial system.[87] Besides, micrometric sized particles detected by SEM images analysis, did not affect the biological activity of entrapped INS.

4. Conclusions

Nanodrying technology is often described as a versatile operating system. In this work, nanodrying technology was successfully employed to obtain INS-CS NP from mixed INS-CS solutions at pH 3, value which is far from the range of pH at which electrostatic interactions would be favored. The pH of the re-hydrated system played a critical role in the INS-CS NP size. At pH < 6, particles tended to be smaller with a highest and positive ζ-potential. In this sense, SEM images of particle size distribution showed a majority of submicrometric particles with a striated rough surface, which would increase the particles dispersibility. A glassy NP powder was obtained, indicating that CS provides a physical thermoprotective matrix for the peptide hormone. FTIR spectra for INS-CS NP highlighted the interaction between INS and CS chemical groups, which were promoted in the feeding solution by hydrophobics and/or hydrogen bounds and to a lesser extent by electrostatic type interactions, and during the dehydration process as a consequence of the physical entrapment. The biological assay performed on an *in-vitro* system with 3T3-L1 fibroblasts, manifested a steady increase in time as evaluated by the phosphorylation of AKT.

The development of new forms for INS administration, such as the pulmonary route, would help to avoid the injury caused by daily injections in the case of patients who require it, especially for the pediatrics ones. CS-INS NP obtained *via* nanospray technology demonstrated to maintain the specific INS functions, increasing their absorption and exerting their controlled release as demonstrated in present work with the biological assay.

Disclosure statement

The authors report no conflicts of interest. The authors are responsible for the contents and writing of this article.

Funding

This research was supported by Projects from Universidad de Buenos Aires (20020150100079BA and 20020170100557BA), ANPCyT (PICT 2017–1683, 2017-1744 and 2015-3866) and CONICET, Argentina.

References

[1] Syed Mohamad Al-Azi, S. O.; Tan, Y. T. F.; Wong, T. W. Transforming Large Molecular Weight Pectin and Chitosan into Oral Protein Drug Nanoparticulate Carrier. *React. Funct. Polym.* **2014**, *84*, 45–52. DOI: 10.1016/j.reactfunctpolym.2014.09.005.

[2] Drosou, C. G.; Krokida, M. K.; Biliaderis, C. G. Encapsulation of Bioactive Compounds through Electrospinning/Electrospraying and Spray Drying: A Comparative Assessment of Food-Related Applications. *Dry. Technol.* **2017**, *35*, 139–162. DOI: 10.1080/07373937.2016.1162797.

[3] Đorđević, V.; Balanč, B.; Belščak-Cvitanović, A.; Lević, S.; Trifković, K.; Kalušević, A.; Kostić, I.; Komes, D.; Bugarski, B.; Nedović, V. Trends in Encapsulation Technologies for Delivery of Food Bioactive Compounds. *Food Eng. Rev.* **2014**, *7*, 1107–1121. DOI: 10.1007/s12393-014-9106-7.

[4] Estevinho, B. N.; Rocha, F.; Santos, L.; Alves, A. Microencapsulation with Chitosan by Spray Drying for Industry Applications - A Review. *Trends Food Sci. Technol.* **2013**, *31*, 138–155. DOI: 10.1016/j.tifs.2013.04.001.

[5] Gharsallaoui, A.; Roudaut, G.; Chambin, O.; Voilley, A.; Saurel, R. Applications of Spray-Drying in Microencapsulation of Food Ingredients: An Overview. *Food Res. Int.* **2007**, *40*, 1107–1121. DOI: 10.1016/j.foodres.2007.07.004.

[6] Lorenzo-Lamosa, M. L.; Remunan-Lopez, C.; Vila-Jato, J. L.; Alonso, M. J. Design of Microencapsulated Chitosan Microspheres for Colonic Drug Delivery. J. Control. Release **1998**, *52*, 109–118. DOI: 10.1016/S0168-3659(97)00203-4.

[7] Berger, J.; Reist, M.; Mayer, J. M.; Felt, O.; Peppas, N. A.; Gurny, R. Structure and Interactions in Covalently and Ionically Crosslinked Chitosan Hydrogels for Biomedical Applications. Eur. J. Pharm. Biopharm. **2004**, *57*, 19–34. DOI: 10.1016/S0939-6411(03)00161-9.

[8] Sarabandi, K.; Gharehbeglou, P.; Jafari, S. M. Spray-Drying Encapsulation of Protein Hydrolysates and Bioactive Peptides: Opportunities and Challenges. *Dry. Technol.* **2020**, *38*, 577–595. DOI: 10.1080/07373937.2019.1689399.

[9] Schmid, K.; Arpagaus, C.; Friess, W. Evaluation of the Nano Spray Dryer B-90 for Pharmaceutical Applications Evaluation of the Nano Spray Dryer B-90 for Pharmaceutical Applications. *Pharm Dev Technol.* **2011**, *29*, 7450. 10.3109/10837450.2010.485320.

[10] Arpagaus, C.; Meuri, M. Laboratory Scale Spray Drying of Inhalable Particles : A Review. *Respir. Drug Deliv.* **2010**, *168*, 469–476.

[11] Dimer, F. A.; Ortiz, M.; Pohlmann, A. R.; Guterres, S. S. Journal of Drug Delivery Science and Technology Inhalable Resveratrol Microparticles Produced by Vibrational Atomization Spray Drying for Treating Pulmonary Arterial Hypertension. *J. Drug Deliv. Sci. Technol.* **2015**, *29*, 152–158. DOI: 10.1016/j.jddst.2015.07.008.

[12] Pérez-Masiá, R.; López-Nicolás, R.; Periago, M. J.; Ros, G.; Lagaron, J. M.; López-Rubio, A. Encapsulation of Folic Acid in Food Hydrocolloids through Nanospray Drying and Electrospraying for Nutraceutical Applications. *Food Chem.* **2015**, *168*, 124–133. DOI: 10.1016/j.foodchem.2014.07.051.

[13] Veneranda, M.; Hu, Q.; Wang, T.; Luo, Y.; Castro, K.; Madariaga, M. Formation and Characterization of Zein-Caseinate-Pectin Complex Nanoparticles for Encapsulation of Eugenol. *LWT - Food Sci. Technol.* **2018**, *89*, 596–603. DOI: 10.1016/j.lwt.2017.11.040.

[14] Harsha, N. S. In Vitro and in Vivo Evaluation of Nanoparticles Prepared by Nano Spray Drying for Stomach Mucoadhesive Drug Delivery. *Dry. Technol.* **2015**, *33*, 1199–1209. DOI: 10.1080/07373937.2014.995305.

[15] Assadpour, E.; Jafari, S. M. Advances in Spray-Drying Encapsulation of Food Bioactive Ingredients : From Microcapsules to Nanocapsules. *Review Annu. Rev. Food Sci. Technol.* **2019**, *10*, 103–131. DOI: 10.1146/annurev-food-032818-121641.

[16] Feng, A. L.; Boraey, M. A.; Gwin, M. A.; Finlay, P. R.; Kuehl, P. J.; Vehring, R. Mechanistic Models Facilitate Efficient Development of Leucine Containing Microparticles for Pulmonary Drug Delivery. Int. J. Pharm. **2011**, *409*, 156–163. DOI: 10.1016/j.ijpharm.2011.02.049.

[17] Li, X.; Anton, N.; Arpagaus, C.; Belleteix, F.; Vandamme, T. F. Nanoparticles by Spray Drying Using Innovative New Technology: The Büchi Nano Spray Dryer B-90. *J. Control Release* **2010**, *147*, 304–310. DOI: 10.1016/j.jconrel.2010.07.113.

[18] Blasi, P.; A.; Schoubben, S.; Giovagnoli, C. R.; M. R. Alginate Micro- and Nanoparticle Production by Spray Drying. In *Meeting on Lactose as a Carrier for Inhalation Products*; Products, M. on lactose as a carrier for inhalation, Ed.; Meeting on lactose as a carrier for inhalation products: Parma, **2010**; pp 137–138.

[19] Abdel-Mageed, H. M.; Fouad, S. A.; Teaima, M. H.; Azza, M.; Fahmy, A. S.; Shaker, D. S.; Mohamed, S. A.; Fouad, S. A.; Teaima, M. H.; Abdel-Aty, A. M. Optimization of Nano Spray Drying Parameters for Production of α -Amylase Nanopowder for Biotheraputic Applications Using Factorial Design. *Dry. Technol.* **2019**, *37*, 2152–2160. DOI: 10.1080/07373937.2019.1565576.

[20] Shukla, S. K.; Mishra, A. K.; Arotiba, O. A.; Mamba, B. B. Chitosan-Based Nanomaterials: A State-of-the-

Art Review. *Int. J. Biol. Macromol.* **2013**, *59*, 46–58. DOI: 10.1016/j.ijbiomac.2013.04.043.

[21] Fonte, P.; Araújo, F.; Silva, C.; Pereira, C.; Reis, S.; Santos, H. a.; Sarmento, B. Polymer-Based Nanoparticles for Oral Insulin Delivery: Revisited Approaches. *Biotechnol. Adv.* **2015**. 10.1016/j.biotechadv.2015.02.010.

[22] Hu, X.; Jiang, M.; Wang, J.; Zhu, L.; Zheng, S.; Snavely, W. K.; Hong, Y.; Su, Y.; Wang, H.; Li, J. Insulin and Insulin–Tripalmitin Particles Produced by a Supercritical Assisted Drying Process. *Dry. Technol.* **2013**, *31*, 1837–1848. DOI: 10.1080/07373937.2013.829852.

[23] Deshmukh, R.; Wagh, P.; Naik, J. Solvent Evaporation and Spray Drying Technique for Micro- and Nanospheres/Particles Preparation: A Review. *Dry. Technol.* **2016**, *34*(15), 1758–1772. DOI: 10.1080/07373937.2016.1232271.

[24] Islam, N.; Ferro, V. Recent Advances in Chitosan-Based Nanoparticulate Pulmonary Drug Delivery. *Nanoscale* **2016**, *8*, 14341–14358. DOI: 10.1039/c6nr03256g.

[25] Prudkin Silva, C.; Martínez, J. H.; Martínez, K. D.; Farías, M. E.; Leskow, F. C.; Pérez, O. E. Proposed Molecular Model for Electrostatic Interactions between Insulin and Chitosan. Nano-Complexation and Activity in Cultured Cells. *Colloids Surfaces A Physicochem. Eng. Asp.* **2018**, *537*, 425–434. DOI: 10.1016/j.colsurfa.2017.10.040.

[26] Tian, H.; He, Z.; Sun, C.; Yang, C.; Zhao, P.; Liu, L.; Leong, K. W.; Mao, H.; Liu, Z.; Chen, Y. Uniform Core – Shell Nanoparticles with Thiolated Hyaluronic Acid Coating to Enhance Oral Delivery of Insulin. *Adv. Healthcare Mater.* **2018**, *7*, 1800285, 1–12. DOI: 10.1002/adhm.201800285.

[27] Kim, N. A.; Thapa, R.; Jeong, S. H.; Bae, H.; Maeng, J.; Lee, K.; Park, K. Enhanced Intranasal Insulin Delivery by Formulations and Tumor Protein-Derived Protein Transduction Domain as an Absorption Enhancer. *J Control Release* **2019**, *294*, 226–236. DOI: 10.1016/j.jconrel.2018.12.023.

[28] Cal, K.; Sollohub, K. Spray Drying Technique. I: Hardware and Process Parameters. J. Pharm. Sci. **2010**, *99*, 575–586. DOI: 10.1002/jps.21886.

[29] Murueva, A. V.; Shershneva, A. M.; Abanina, K. V.; Prudnikova, S. V.; Shishatskaya, E. I. Development and Characterization of Ceftriaxone-Loaded P3HB-Based Microparticles for Drug Delivery. *Dry. Technol.* **2019**, *37*, 1131–1142. DOI: 10.1080/07373937.2018.1487451.

[30] Pérez, O. E.; David-Birman, T.; Kesselman, E.; Levi-Tal, S.; Lesmes, U. Milk Protein–Vitamin Interactions: Formation of Beta-Lactoglobulin/Folic Acid Nano-Complexes and Their Impact on in Vitro Gastro-Duodenal Proteolysis. *Food Hydrocoll.* **2014**, *38*, 40–47. DOI: 10.1016/j.foodhyd.2013.11.010.

[31] Horiba. A Guidebook To Particle Size Analysis. **2016**.

[32] Stirpe, A.; Pantusa, M.; Rizzuti, B.; Sportelli, L.; Bartucci, R.; Guzzi, R. Early Stage Aggregation of Human Serum Albumin in the Presence of Metal Ions. *Int. J. Biol. Macromol.* **2011**, *49*, 337–342. DOI: 10.1016/j.ijbiomac.2011.05.011.

[33] Alvarado-Palacios, Q. G.; San Martin-Martinez, E.; Gomez-García, C.; Estanislao-Gomez, C. C.; Casañas-Pimentel, R. Nanoencapsulation of the Aranto (Kalanchoe Daigremontiana) Aquoethanolic Extract by Nanospray Dryer and Its Selective Effect on Breast Cancer Cell Line. *Int. J. Pharmacogn. Phytochem. Res.* **2015**, *7*, 888–895.

[34] Thandapani, G.; Supriya Prasad, P.; Sudha, P. N.; Sukumaran, A. Size Optimization and in Vitro Biocompatibility Studies of Chitosan Nanoparticles. *Int. J. Biol. Macromol.* **2017**, *104*, 1794–1806. DOI: 10.1016/j.ijbiomac.2017.08.057.

[35] Pan, Y.; Li, Y-j.; Zhao, H-y.; Zheng, J-m.; Xu, H.; Wei, G.; Hao, J-s.; Cui, F-d. Bioadhesive Polysaccharide in Protein Delivery System. *Pdf* **2002**, *249*, 139–147. DOI: 10.1016/S0378-5173(02)00486-6.

[36] Leonida, M.; Belbekhouche, S.; Adams, F.; Bijja, U. K.; Choudhary, D. A.; Kumar, I. Enzyme Nanovehicles: Histaminase and Catalase Delivered in Nanoparticulate Chitosan. Int. J. Pharm. **2019**, *557*, 145–153. DOI: 10.1016/j.ijpharm.2018.12.050.

[37] Mukhopadhyay, P.; Sarkar, K.; Chakraborty, M.; Bhattacharya, S.; Mishra, R.; Kundu, P. P. Oral Insulin Delivery by Self-Assembled Chitosan Nanoparticles: In Vitro and in Vivo Studies in Diabetic Animal Model. *Mater. Sci. Eng. C Mater. Biol. Appl.* **2013**, *33*, 376–382. DOI: 10.1016/j.msec.2012.09.001.

[38] dos Santos, C.; Buera, M. P.; Mazzobre, M. F. Phase Solubility Studies and Stability of Cholesterol/β-Cyclodextrin Inclusion Complexes. *J. Sci. Food Agric.* **2011**, *91*, 2551–2557. DOI: 10.1002/jsfa.4425.

[39] Liao, Y.; Hung, M. C. Physiological Regulation of Akt Activity and Stability. *Am. J. Transl. Res.* **2010**, *2*, 19–42.

[40] Alaimo, A.; Gorojod, R. M.; Beauquis, J.; Muñoz, M. J.; Saravia, F.; Kotler, M. L. Deregulation of Mitochondria-Shaping Proteins Opa-1 and Drp-1 in Manganese-Induced Apoptosis. *PLoS One.* **2014**, *9*, e91848. DOI: 10.1371/journal.pone.0091848.

[41] Prudkin-Silva, C.; Pérez, O. E.; Martínez, K. D.; Barroso Da Silva, F. L. Combined Experimental and Molecular Simulation Study of Insulin-Chitosan Complexation Driven by Electrostatic Interactions. *J. Chem. Inf. Model.* **2020**, *60*, 854–865. DOI: 10.1021/acs.jcim.9b00814.

[42] Grotz, E.; Tateosian, N. L.; Salgueiro, J.; Bernabeu, E.; Gonzalez, L.; Manca, M. L.; Amiano, N.; Valenti, D.; Manconi, M.; García, V.; et al. Pulmonary Delivery of Rifampicin-Loaded Soluplus Micelles against Mycobacterium Tuberculosis. *J. Drug Deliv. Sci. Technol.* **2019**, *53*, 101170. DOI: 10.1016/j.jddst.2019.101170.

[43] Yang, J.; Han, S.; Zheng, H.; Dong, H.; Liu, J. Preparation and Application of Micro/Nanoparticles Based on Natural Polysaccharides. Carbohydr. Polym. **2015**, *123*, 53–66. DOI: 10.1016/j.carbpol.2015.01.029.

[44] Yang, X. F.; Xu, Y.; Qu, D. S.; Li, H. Y. The Influence of Amino Acids on Aztreonam Spray-

Dried Powders for Inhalation. *Asian J. Pharm. Sci* **2015**, *10*, 541–548. DOI: 10.1016/j.ajps.2015.08.002.

[45] Penalva, R.; Esparza, I.; Agüeros, M.; Gonzalez-Navarro, C. J.; Gonzalez-Ferrero, C.; Irache, J. M. Casein Nanoparticles as Carriers for the Oral Delivery of Folic Acid. *Food Hydrocoll.* **2015**, *44*, 399–406. DOI: 10.1016/j.foodhyd.2014.10.004.

[46] O'Toole, M. G.; Henderson, R. M.; Soucy, P. A.; Fasciotto, B. H.; Hoblitzell, P. J.; Keynton, R. S.; Ehringer, W. D.; Gobin, A. S. Curcumin Encapsulation in Submicrometer Spray-Dried Chitosan/Tween 20 Particles. *Biomacromolecules* **2012**, *13*, 2309–2314. DOI: 10.1021/bm300564v.

[47] Ngan, L. T. K.; Wang, S. L.; Hiep, I. M.; Luong, P. M.; Vui, N. T.; Crossed, D.; Signinh, T. M.; Dzung, N. A. Preparation of Chitosan Nanoparticles by Spray Drying, and Their Antibacterial Activity. Res. Chem. Intermed. **2014**, *40*, 2165–2175. DOI: 10.1007/s11164-014-1594-9.

[48] Demir, G. M.; Degim, I. T. Preparation of Chitosan Nanoparticles by Nano Spray Drying Technology. *Fabad J. Pharm. Sci.* **2013**, *38*, 127–133.

[49] Lee, S. H.; Heng, D.; Ng, W. K.; Chan, H. K.; Tan, R. B. H. Nano Spray Drying: A Novel Method for Preparing Protein Nanoparticles for Protein Therapy. Int. J. Pharm. **2011**, *403*, 192–200. DOI: 10.1016/j.ijpharm.2010.10.012.

[50] Cheema, M.; Mohan, M. S.; Campagna, S. R.; Jurat-Fuentes, J. L.; Harte, F. M. The Association of Low-Molecular-Weight Hydrophobic Compounds with Native Casein Micelles in Bovine Milk. *J. Dairy Sci.* **2015**, *98*, 5155–5163. DOI: 10.3168/jds.2015-9461.

[51] Ochnio, M.; Martínez, J.; Allievi, M.; Palavecino, M.; Martínez, K.; Pérez, O. Proteins as Nano-Carriers for Bioactive Compounds. The Case of 7S and 11S Soy Globulins and Folic María Emilia Ochnio 1,†, Jimena H Martínez 2,†, Mariana C Allievi 2, Marcos Palavecino 2, Karina D. Martínez 3,* and Oscar E. Pérez 1,*. *Polymers (Basel)*, **2018**, *10*, 149. DOI: 10.3390/polym10020149.

[52] McClements, D. J. *Food Emulsions: Principles, Practices, and Techniques*; Boca Raton, FL: CRC Press, **2015**.

[53] Le Brun, V.; Friess, W.; Bassarab, S.; Mühlau, S.; Garidel, P. A Critical Evaluation of Self-Interaction Chromatography as a Predictive Tool for the Assessment of protein-protein interactions in protein formulation development: a case study of a therapeutic monoclonal antibody. Eur. J. Pharm. Biopharm. **2010**, *75*, 16–25. DOI: 10.1016/j.ejpb.2010.01.009.

[54] Arpagaus, C. A Novel Laboratory-Scale Spray Dryer to Produce Nanoparticles. *Dry. Technol.* **2012**, *30*, 1113–1121. DOI: 10.1080/07373937.2012.686949.

[55] Jiang, W. Z.; Cai, Y.; Li, H. Y. Chitosan-Based Spray-Dried Mucoadhesive Microspheres for Sustained Oromucosal Drug Delivery. *Powder Technol.* **2017**, *312*, 124–132. DOI: 10.1016/j.powtec.2017.02.021.

[56] Rampino, A.; Borgogna, M.; Blasi, P.; Bellich, B.; Cesàro, A. Chitosan Nanoparticles: Preparation, Size Evolution and Stability. Int. J. Pharm. **2013**, *455*, 219–228. DOI: 10.1016/j.ijpharm.2013.07.034.

[57] Chan, H. K. Dry Powder Aerosol Drug Delivery-Opportunities for Colloid and Surface Scientists. *Colloids Surfaces A Physicochem. Eng. Asp.* **2006**, *284-285*, 50–55. DOI: 10.1016/j.colsurfa.2005.10.091.

[58] Barth, A. Infrared Spectroscopy of Proteins. *Biochim. Biophys. Acta.* **2007**, *1767*, 1073–1101. DOI: 10.1016/j.bbabio.2007.06.004.

[59] Guo, L.; Liu, G.; Hong, R. Y.; Li, H. Z. Preparation and Characterization of Chitosan Poly(Acrylic Acid) Magnetic Microspheres. Mar. Drugs. **2010**, *8*, 2212–2222. DOI: 10.3390/md8072212.

[60] Venkatesham, M.; Ayodhya, D.; Madhusudhan, A.; Veera Babu, N.; Veerabhadram, G. A Novel Green One-Step Synthesis of Silver Nanoparticles Using Chitosan: Catalytic Activity and Antimicrobial Studies. Appl. Nanosci. **2014**, *4*, 113–119. DOI: 10.1007/s13204-012-0180-y.

[61] Heuser, M.; Cárdenas, G. Chitosan-Copper Paint Types as Antifouling. *J. Chil. Chem. Soc.* **2014**, *59*, 2415–2419. DOI: 10.4067/S0717-97072014000200004.

[62] Ramírez Barragán, C. A.; Delgado Fornué, E.; Andrade Ortega, J. A. Determinación Del Grado de Desacetilación de Quitosana Mediante Titulación Potenciométrica, FTIR y Raman. *Coloq. Investig. Multidiscip.* **2016**, *4*, 769–776.

[63] Boonsongrit, Y.; Mueller, B. W.; Mitrevej, A. Characterization of Drug-Chitosan Interaction by 1H NMR, FTIR and Isothermal Titration Calorimetry. Eur. J. Pharm. Biopharm. **2008**, *69*, 388–395. DOI: 10.1016/j.ejpb.2007.11.008.

[64] Ahmadi, S.; Sheikh-Zeinoddin, M.; Soleimanian-Zad, S.; Alihosseini, F.; Yadav, H. Effects of Different Drying Methods on the Physicochemical Properties and Antioxidant Activities of Isolated Acorn Polysaccharides. *LWT* **2019**, *100*, 1–9. DOI: 10.1016/j.lwt.2018.10.027.

[65] Kanwate, B. W.; Ballari, R.; V; Kudre, T. G. Influence of Spray-Drying, Freeze-Drying and Vacuum-Drying on Physicochemical and Functional Properties of Gelatin from Labeo Rohita Swim Bladder. *Int. J. Biol. Macromol.* **2019**, *121*, 135–141. DOI: 10.1016/j.ijbiomac.2018.10.015.

[66] Liu, L.; Dai, X.; Kang, H.; Xu, Y.; Hao, W. Structural and Functional Properties of Hydrolyzed/Glycosylated Ovalbumin under Spray Drying and Microwave Freeze Drying. *Food Sci. Hum. Wellness* **2020**, *9*, 80–87. DOI: 10.1016/j.fshw.2020.01.003.

[67] Desai, K. G. H.; Park, H. J. Encapsulation of Vitamin C in Tripolyphosphate Cross-Linked Chitosan Microspheres by Spray Drying. J. Microencapsul. **2005**, *22*, 179–192. DOI: 10.1080/02652040400026533.

[68] Sampaio, C.; de, G.; Frota, L. S.; Magalhães, H. S.; Dutra, L. M. U.; Queiroz, D. C.; Araújo, R. S.; Becker, H.; de Souza, J. R. R.; Ricardo, N. M. P. S.; Trevisan, M. T. S. Chitosan/Mangiferin Particles for Cr(VI) Reduction and Removal. *Int. J. Biol. Macromol.* **2015**, *78*, 273–279. DOI: 10.1016/j.ijbiomac.2015.03.038.

[69] Sinsuebpol, C.; Chatchawalsaisin, J.; Kulvanich, P. Preparation and in Vivo Absorption Evaluation of Spray Dried Powders Containing Salmon Calcitonin Loaded Chitosan Nanoparticles for Pulmonary Delivery. *Drug Des Devel Ther.* **2013**, *7*, 861–873. DOI: 10.2147/DDDT.S47681.

[70] Adamiec, J.; Modrzejewska, Z. Some Structural Properties of Spray-Dried Chitosan Microgranules. *Dry. Technol.* **2005**, *23*, 1601–1611. DOI: 10.1081/DRT-200064989.

[71] Sarmento, B.; Ribeiro, A.; Veiga, F.; Ferreira, D. Development and Characterization of New Insulin Containing Polysaccharide Nanoparticles. *Colloids Surf B Biointerfaces* **2006**, *53*, 193–202. DOI: 10.1016/j.colsurfb.2006.09.012.

[72] Carpenter, J. F.; Prestrelski, S. J.; Dong, A. Application of Infrared Spectroscopy to Development of Stable Lyophilized Protein Formulations. Eur. J. Pharm. Biopharm. **1998**, *45*, 231–238. DOI: 10.1016/S0939-6411(98)00005-8.

[73] Pikal, M. J.; Rigsbee, D. R.; Roy, M. L. Solid State Chemistry of Proteins: I. Glass Transition Behavior in Freeze Dried Disaccharide Formulations of Human Growth Hormone (HGH). J. Pharm. Sci. **2007**, *96*, 2765–2776. DOI: 10.1002/jps.20960.

[74] Giuffrida, S.; Cottone, G.; Cordone, L. Role of Solvent on Protein-Matrix Coupling in MbCO Embedded in Water-Saccharide Systems: A Fourier Transform Infrared Spectroscopy Study. *Biophys. J.* **2006**, *91*, 968–980. DOI: 10.1529/biophysj.106.081927.

[75] Bellavia, G.; Giuffrida, S.; Cottone, G.; Cupane, A.; Cordone, L. Protein Thermal Denaturation and Matrix Glass Transition in Different Protein-Trehalose-Water Systems. *J. Phys. Chem. B* **2011**, *115*, 6340–6346. DOI: 10.1021/jp201378y.

[76] Fernandez-Urrusuno, R.; Calvo, P.; Remunan-Lopez, C.; Vila-Jato, J. L.; Alonso, M. J. Enhancement of Nasal Absorption of Insulin Using Chitosan Nanoparticles. *Pharm. Res.* **1999**, *16*, 1576–1581.

[77] Hu, Q.; Luo, Y. Recent Advances of Polysaccharide-Based Nanoparticles for Oral Insulin Delivery. *Int. J. Biol. Macromol.* **2018**, *120*, 775–782. DOI: 10.1016/j.ijbiomac.2018.08.152.

[78] Calvo, P.; Remu, N-L.; Pez, C.; Vila-Jato, J. L.; Alonso, M. J. Novel Hydrophilic Chitosan-Polyethylene Oxide Nanoparticles as Protein Carriers. *J. Appl. Polym. Sci.* **1997**, *63*, 125–132. DOI: 10.1002/(SICI)1097-4628(19970103)63:1<125::AID-APP13>3.0.CO;2-4.

[79] Pillay, V.; Murugan, K.; Choonara, Y. E.; Kumar, P.; Bijukumar, D.; Du Toit, L. C. Parameters and Characteristics Governing Cellular Internalization and Trans-Barrier Trafficking of nanostructures. Int. J. Nanomedicine. **2015**, *10*, 2191–2206. DOI: 10.2147/IJN.S75615.

[80] Torchilin, V. P. Recent Approaches to Intracellular Delivery of Drugs and DNA and Organelle Targeting. Annu. Rev. Biomed. Eng. **2006**, *8*, 343–375. DOI: 10.1146/annurev.bioeng.8.061505.095735.

[81] Awaad, A.; Nakamura, M.; Ishimura, K. Imaging of Size-Dependent Uptake and Identification of Novel Pathways in Mouse Peyer's patches using fluorescent organosilica particles. *Nanomedicine* **2012**, *8*, 627–636. DOI: 10.1016/j.nano.2011.08.009.

[82] Lee, J.; Pilch, P. F. The Insulin Receptor: Structure, Function, and Signaling. *Am. J. Physiol.* **1994**, *266*, C319–C334. DOI: 10.1152/ajpcell.1994.266.2.C319.

[83] Chen, S.; Xiao, X.; Feng, X.; Li, W.; Zhou, N.; Zheng, L.; Sun, Y.; Zhang, Z.; Zhu, W. Resveratrol Induces Sirt1-Dependent Apoptosis in 3T3-L1 Preadipocytes by Activating AMPK and Suppressing AKT Activity and Survivin Expression. *J. Nutr. Biochem.* **2012**, *23*, 1100–1112. DOI: 10.1016/j.jnutbio.2011.06.003.

[84] Haeusler, R. A.; McGraw, T. E.; Accili, D. Metabolic Signalling: Biochemical and Cellular Properties of Insulin Receptor Signalling. *Nat. Rev. Mol. Cell Biol.* **2018**, *19*, 31–44. DOI: 10.1038/nrm.2017.89.

[85] Dima, C.; Pătraşcu, L.; Cantaragiu, A.; Alexe, P.; Dima, Ş. The Kinetics of the Swelling Process and the Release Mechanisms of Coriandrum Sativum L. Essential Oil from Chitosan/Alginate/Inulin Microcapsules. *Food Chem.* **2016**, *195*, 39–48. DOI: 10.1016/j.foodchem.2015.05.044.

[86] Rahaiee, S.; Hashemi, M.; Shojaosadati, S. A.; Moini, S.; Razavi, S. H. Nanoparticles Based on Crocin Loaded Chitosan-Alginate Biopolymers: Antioxidant Activities, Bioavailability and Anticancer Properties. *Int. J. Biol. Macromol.* **2017**, *99*, 401–408. DOI: 10.1016/j.ijbiomac.2017.02.095.

[87] Damiati, S.; Scheberl, A.; Zayni, S.; Damiati, S. A.; Schuster, B.; Kompella, U. B. Albumin-bound nanodiscs as delivery vehicle candidates: Development and characterization. *Biophys. Chem.* **2019**, *251*, 106178. DOI: 10.1016/j.bpc.2019.106178.